EVALUATION OF THREE SUPERVISED CLASSIFIERS IN MAPPING "DEPTH TO LATE-SUMMER FROZEN GROUND," CENTRAL YUKON TERRITORY

by DAVID W. LEVERINGTON • CLAUDE R. DUGUAY

RÉSUMÉ

Devant les préoccupations croissantes suscitées par les changements climatiques à l'échelle mondiale, un programme de recherche visant à mettre au point des méthodes de surveillance des changements dans la cryosphère à l'aide de données de télédétection comme source principale de données a été mis en oeuvre. Ce programme, connu sous l'appellation CRYSYS (CRYospheric SYStem), porte principalement sur la surveillance des conditions de neige et de glace de surface dans le but de contrôler les processus régis par le climat qui influencent la cryosphère. L'un des constituants de la cryosphère présentant un intérêt particulier est le pergélisol.

Le principal objectif de cette recherche consistait à évaluer trois méthodes de classification dirigée (maximum de vraisemblance, raisonnement d'évidence et réseau neuronal) pour la prévision et la cartographie de la profondeur de pénétration du gel en fin d'été (PPG) dans la zone étendue de pergélisol discontinu de la forêt boréale au coeur du Yukon. L'imagerie utilisée dans les classifications se composait de données recueillies par le capteur thématique de Landsat et de données dérivées d'un modèle numérique d'élévation, connues pour être corrélées avec le PPG. Les résultats d'une analyse à deux classes démontrent que tous les classificateurs soumis à l'analyse permettent de générer des résultats satisfaisants dans le région de Mayo. Le classificateur fondé sur la méthode des réseaux neuronaux est celui qui a donné les meilleurs résultats, à savoir un taux de concordance de 93 % entre les deux classes définies, soit à partir des images, soit à partir des relevés de terrain. Les données relatives à la couverture du sol et à la latitude équivalente se sont révélées particulièrement utiles dans les classifications. Lorsque trois classes de PPG ont été définies, des taux de concordance nettement inférieurs ont été obtenus pour tous les classificateurs, ce qui corroborent les observations de terrain selon lesquelles il n'existe que deux classes de PPG dans la région à l'étude.

SUMMARY

With increased concern about the nature of global climate change, a program has been established to develop techniques for monitoring changes in cryosphere parameters using remotely sensed data as a primary data source. This research program, known as CRYSYS (CRYospheric SYStem), is focussing on monitoring surface snow and ice conditions in order to monitor climate-driven processes that influence the cryosphere. One component of the cryosphere that is of particular interest is permafrost. The primary objective of this research was to evaluate three supervised classification schemes (maximum likelihood, evidential reasoning, and a neural network) in the prediction and mapping of depth to late-summer frozen ground (DTFG) in the widespread discontinuous permafrost zone of the boreal forest of central Yukon. Source imagery used in the classifications was composed of TM- and DEM-derived data known to be correlated with DTFG. Results of a two-class DTFG experiment indicate that all tested classifiers are suitable for generating two-class correlative DTFG data products in the Mayo region. The neural network classifier was found to be most successful, producing a two-class DTFG image with a 93% agreement rate between predicted and field-measured DTFG classes. Land cover

• David W. Leverington and Claude R. Duguay are with the Ottawa-Carleton Geoscience Centre, University of Ottawa, Ottawa, Ontario K1N 6N5.

and equivalent latitude were consistently found to be especially useful sources for use in the classifications. When three DTFG classes were used, agreement rates greatly decreased for all classifiers, supporting field observations that suggest that only two DTFG classes exist in the study area.

INTRODUCTION

Approximately half of Canada is underlain by permafrost (NRC, 1988). Because the distribution of permafrost is primarily a function of climate, the monitoring of permafrost conditions and geographic extent could be a useful means of deriving information concerning global climate change. With high-latitude regions being remote and vast in scale, they can most effectively be investigated using satellite remote sensing. Unfortunately, permafrost cannot be directly observed by orbiting sensors in the way that exposed cryosphere elements such as snow cover, sea ice cover, or glacier extent can be. Permafrost is a sub-surface phenomenon, and its extent in the discontinuous permafrost zone can be derived by correlating ground ice conditions with various geophysical factors. There is currently a need to develop remote sensing techniques for the purpose of extracting and mapping near-surface permafrost conditions, and for monitoring changes in permafrost conditions over time.

A research program has been established to monitor and predict physical impacts on the cryosphere of predicted global warming in northern regions of Canada using mainly remote sensing observations. CRYSYS (CRYospheric SYStem to monitor global change in Canada) is a program within NASA's Earth Observing System (EOS), and is a key component of the Canadian Global Change Program. The two scientific goals of the EOS CRYSYS project are to:

- monitor the Earth system changes in Canada as manifested by cryospheric variables, such as snow, glaciers and ice caps, lake and river ice, sea ice, and permafrost; and
- predict global warming effects on the cryosphere at regional and polar scale (CRYSYS Steering Committee, 1991).

The scientific questions currently being addressed as part of the permafrost component of CRYSYS are:

- What is the relationship between surface properties directly related to permafrost, such as surface temperature, near surface ground ice, thermokarst subsidence, and active-layer depth, and remotely sensed data?
- What is the relationship between surface properties indirectly related to permafrost, such as snow cover, vegetation, and surface hydrology, and remotely sensed data?
- What is the most effective combination of data products that could be derived from EOS instruments for extracting permafrost conditions?
- Can these techniques be validated for diverse test areas throughout polar regions?
- How can these techniques handle changes in permafrost conditions over large areas and be used to monitor global climate change?

In this study, known correlative relationships between surface properties and permafrost were used to determine effective combinations of image classifiers and data sources for the extraction of "late-summer depth to frozen ground" (DTFG) classes. Late-summer DTFG closely approximates active-layer thickness, a variable of interest both to Earth scientists and engineers. More specifically, maximum likelihood (ML), evidential reasoning (ER), and neural network (NN) classifiers were evaluated in their ability to predict late-summer DTFG in the boreal forest of central Yukon using Landsat TM and digital terrain data.

BACKGROUND

Permafrost is soil or rock that has remained cryotic (at or below 0°C) for a minimum of two years (NRC, 1988). The active layer is the layer of ground in areas underlain by permafrost that is subject to annual freezing and thawing. Climate is the dominant factor influencing the continental distribution of permafrost, generally resulting in an increase in permafrost occurrence and thickness with increasing latitude. In areas where permafrost occurrence is discontinuous, the large-scale distribution of permafrost is strongly influenced by local microclimate factors, such as slope, aspect, local hydrology, vegetation cover, geology, and snow cover (Hall and Martinec, 1985; Ferrians and Hobson, 1973; Williams and Smith, 1989). Permafrost and active-layer conditions, involving sub-surface ground materials, cannot be imaged using airborne or satellite-based sensors. Therefore, near-surface permafrost conditions must be indirectly deduced from other related microclimate factors that can be detected using remote sensing techniques (Tarnocai and Thie, 1974a; Hall and Martinec, 1985; Morrissey, 1984).

Early efforts in permafrost mapping and characterization were made using Landsat MSS imagery (see, for example, Anderson *et al.*, 1973; Tarnocai and Thie, 1974b). The spatial and spectral resolution of MSS (80 m and four spectral bands), coupled with limitations in digital image processing techniques, resulted in unsatisfactory digital permafrost maps. Nevertheless, the qualitative detection of large permafrost-related landscape features such as peat plateaus was found to be easily performed using Landsat MSS data (Tarnocai and Thie, 1974b).

Improvements in the spatial and spectral resolution of satellite imagery have resulted in the development of procedures for use in near-surface active-layer and permafrost mapping. For example, Morrissey *et al.* (1986) prepared maps of near-surface permafrost conditions in a 106 km^2 area in Alaska using various combinations of three variables as input to logistic discriminant functions: equivalent latitude, a Landsat TM-derived vegetation map, and TM band 6. The highest classification accuracy (78%) was obtained using the TM thermal data and the TM-derived vegetation

classification. An accuracy of 75.5% was obtained using equivalent latitude and the TM vegetation classification. Lower accuracies ranging between 62% and 70% were achieved using each of the three input variables alone. Unfortunately, the permafrost classes used in the study are not particularly useful: class 1: 95–100% frozen (by area); class 2: 6–94% frozen; and class 3: 0–5% frozen. Using SPOT HRV and digital terrain data, Peddle and Franklin (1993) were able to predict four early-summer frozen ground classes within a 100 km^2 study site in the Ruby Range, Yukon Territory, based on land cover, terrain aspect, and equivalent latitude and using an evidential reasoning classifier. The four frozen ground classes used in the study were: class 1: < 25 cm; class 2: 25–50 cm; class 3: > 50 cm; and 4: an absent class. A classification accuracy of 79% was obtained based on evidence generated from the remotely sensed information listed above. A classification accuracy of 87% was later produced with a neural network classifier (Peddle *et al.*, 1994).

Although these results demonstrate the potential utility of multi-source classifications for permafrost mapping, further work is necessary if prediction procedures are to be used in such operational programs as EOS CRYSYS. The present research focused on determining the utility of three classifiers in the production of two- and three-class DTFG imagery near Mayo, Yukon Territory. Special attention was given to the field component of this study. Depth to frozen ground was measured in late summer, and over as short a period as possible, in order to best approximate active-layer thicknesses; only through late-summer field sampling can permafrost be differentiated from seasonally frozen ground. Furthermore, DTFG data were sampled over the widest possible variety of environments within the study area. A complete field effort is a prerequisite in the generation of accurate DTFG imagery.

STUDY AREA AND DATA COLLECTION

Study Area

The study area was chosen as a "target region" by the CRYSYS Steering Committee (1991). It is located in the Central Yukon Basin, and lies in the boreal forest and widespread discontinuous permafrost zone (**Figure 1**). The 18 km by 18 km study area is bounded along its northern and southern limits by east-west oriented hills that enclose Stewart River, which runs west across the centre of the study site. Elevations range from approximately 500 m ASL in the Stewart River Valley to 1200 m ASL in hills to the north.

The study area is underlain by quartzite, argillite, shale, and phyllite (Bostock, 1946; Gabrielse *et al.*, 1980) and is within the limits of the Late-Wisconsin Reid and McConnell advances of the Pleistocene Cordilleran Ice Sheet (Bostock 1966; Burn, 1985; Hughes, 1983; Hughes *et al.*, 1989). Quaternary sediments blanket much of the Stewart River Valley, and bedrock is exposed only on especially steep slopes. Valley deposits include alluvial and glaciolacustrine sediments, while hillside deposits consist of colluvium and till (Hughes, 1983).

The climate of the region is continental: precipitation is relatively moderate and temperatures approach extreme values both in the summer and winter. The mean annual air temperature at Mayo is -4°C, mean annual rainfall is 185 mm, and mean annual snowfall is 131 cm (Wahl *et al.*, 1987).

The region's coniferous forests are composed of both Black spruce (*Picea mariana*) and White spruce (*Picea glauca*). Black spruce is more likely to dominate coniferous stands located on poorly drained soils, as is typical of this species (see, for example, Scott, 1995). Deciduous stands are composed primarily of the following three species: Balsam poplar (*Populus basamifera*), Trembling aspen (*Populus tremuloides*), and Paper birch (*Betula papyrifera*). Willows (*Salix* spp.) tend to dominate especially wet and poorly drained zones. Feathermosses and *Sphagnum* spp. are commonly well represented in the surface biomass of coniferous forest sites throughout the region, and have in the past contributed to the thick accumulation of dead organic matter at many such sites. An account of typical vegetation species found in the Mayo area is given in Burn and Friele (1989).

The study area is ideal for testing image classifiers and a multi-source dataset:

- it contains a variety of slopes, aspects, and elevations;
- it is topographically representative of much of the Mayo region, containing valley bottom, valley side, and tableland units;
- it is underlain by a variety of surface deposits, ranging from glaciolacustrine, glaciofluvial, and alluvial valley deposits to morainal and colluvial deposits on most slopes; and
- it is representative of the general boreal forest ecosystem of the Mayo region, containing a wide range of land cover types.

Permafrost Conditions in the Mayo Region

Regional topographic effects associated with the mountains of the western Cordillera maintain the severe winter temperatures and low winter snowfall that favour the maintenance of permafrost in the valleys of southern and central Yukon and the Upper Mackenzie District (Burn, 1994). In the widespread discontinuous permafrost zone, the occurrence of permafrost is difficult to predict with certainty, not always being restricted to a particular simple set of terrain types; the interrelation of various natural factors contributes to variations in the occurrence and extent of permafrost. Nevertheless, in central Yukon, permafrost is often found on north-facing slopes vegetated by spruce trees and extensive moss cover, whereas south-facing slopes are usually not associated with permafrost and are vegetated by deciduous trees (Brown, 1967). Permafrost is usually not associated with areas of deep snow accumulation, and low wet areas in which bodies of water have been filled in recently. Permafrost is extensive in the valleys of central Yukon, where permafrost thicknesses can range between 30 and 40 m in areas where Holocene surface erosion has not occurred (Burn, 1991).

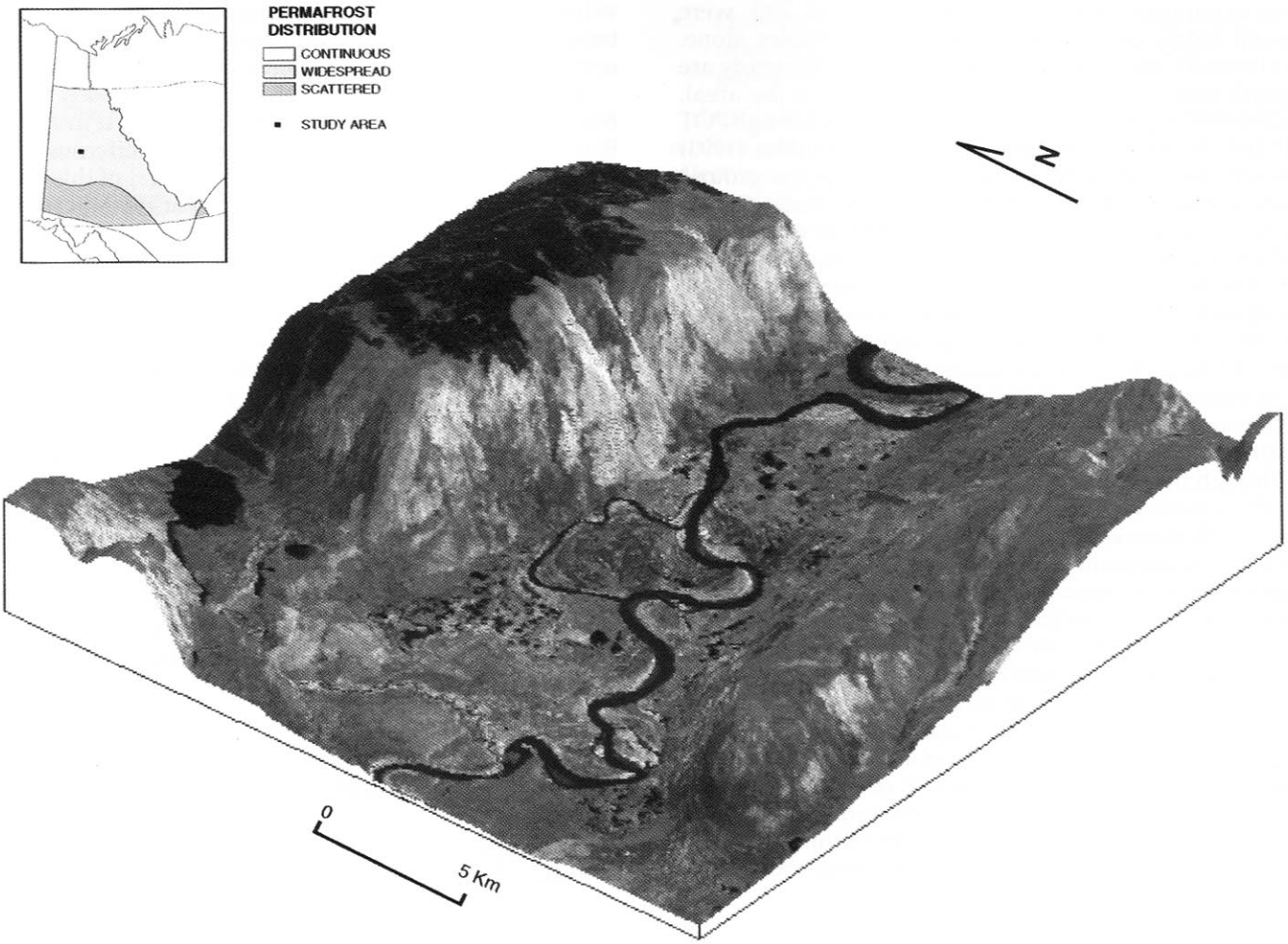

Figure 1.
Mayo study area, central Yukon. The location of the Mayo study area in reference to a generalized permafrost distribution map of Yukon is shown in the upper left corner (after Brown, 1978). Also shown is the Landsat TM band 4 (August 6, 1990) draped over the coregistered DEM of the study area. Vertical exaggeration is 10x.

Burn (1991) found permafrost thickness in alluvial sediments near Mayo to be ~20 m, while permafrost thickness at the Mayo Group Home, east of Mayo, is 37 m. A summary of recent borehole measurements associated with construction at Mayo indicates that depth to the permafrost table can range from ~0.6 to 13.5 m at sites near the settlement (Burn, 1991). September active-layer depth measured at forest sites located 3 km south-east of Mayo in glaciolacustrine silty clay have been measured to range between ~35 cm and 100 cm (Burn and Friele, 1989). Measurements made by Burn and Smith (1990) indicate that near-surface permafrost in glaciolacustrine sediments near Mayo are ice-rich, with measured volumetric ice contents of up to 80%. A full description of permafrost conditions near Mayo is given in Leverington (1995a).

Landsat Thematic Mapper Data

TM imagery was selected because of its pixel size, which roughly corresponds to the accuracy of site positioning. Bands 3, 4, and 5 were selected as ideal due to their applicability in the differentiation of vegetative communities and general land cover (Beaubien, 1994). The TM image used here was geometrically corrected and georeferenced to a UTM projection using 18 GCPs. Nearest neighbour resampling was used to retain original pixel brightnesses. The root mean square of the residuals in both directions (Easting and Northing) were 0.46 and 0.48, respectively.

A sub-scene of the study area was extracted from the geometrically corrected TM image. A land cover image was generated through a Maximum Likelihood (ML) classification of the TM imagery using training sites based on 1993 and 1994 fieldwork. Land cover classes include: mature spruce forest; low and open spruce forest; very open spruce

forest; other spruce forest; mixed deciduous and coniferous forest; light deciduous forest (that is, bright deciduous forest on imagery due to slope effects, etc.); dark deciduous forest; exposed sand and concrete; river sandbar; recent burn; turbid water; clear water; and reservoir water. The extensive division of the spruce forest, deciduous forest, and water classes was necessary due to the inability of the ML classifier to operate with multi-modal class signatures. A full description of the creation of the land cover image is given in Leverington (1995b).

A Normalized Difference Vegetation Index (NDVI) image was also generated as a secondary land cover source, since land cover imagery cannot usually be used as input to the ML classifier. Photosynthetically active plant components such as leaves have a low reflectance in the visible and high reflectance in the infrared. The NDVI index is thus strongly related to such variables as the leaf area of plant canopies, and is a general indicator of ecosystem type. The NDVI is influenced by such factors as canopy closure and density, understorey type and density, and the presence of water or rock outcrops (Cihlar *et al.*, 1991).

Topography

The topography of the area was digitized from NTS map 105 M/12 (1:50 000) using PC ARC/INFO. The DEM was generated from the digitized map using PC ARC/TIN, and then converted to raster format with 30 m pixels to correspond to the TM image resolution. Images of slope, aspect, and equivalent latitude were derived from the DEM. Equivalent latitude was calculated based on the equation used by Morrissey *et al.* (1986):

$$\theta' = \sin^{-1} (\sin k \cos h \cos\theta + \cos k \sin\theta) \quad (1)$$

where k is the slope of the surface, h is the aspect of the surface, θ is the actual latitude of the area, and θ' is the equivalent latitude of the surface.

Field Data

Between July 19 and August 29, 1994, 325 field sites were visited. An additional 35 field sites with known thawed conditions within 1.5 m of ground surface were added after the field season to ensure complete coverage of all otherwise unrepresented land cover types in the study site's field dataset; additional sites included concrete, sand pit, and beach sand land covers.

In general, DTFGs in the Mayo area approach their maximum by mid to late July (C. Burn, personal communication, 1994). As a result, the 1994 field measurements were made in late summer so that DTFG values would approximate active-layer thicknesses. Most areas suspected to have thick active layers (>1.5 m, or absent) were sampled first, allowing thinner active layers (those most sensitive to premature measurement) to be sampled as late as possible in the field season.

General site selections were made in advance of the 1994 field season based on aerial photography and a sampling procedure stratified by predominant land cover, topography, and surface geology. The precise locations of sites were necessarily determined *in situ*. Key information obtained at each site included: land cover (mature Black spruce forest, for example); DTFG (measured in pits and with a probe); site coordinates; and additional information of interest (ground material, estimated tree heights, slope and aspect, surface exposure). Site coordinates were derived using recent visible and near-infrared black-and-white aerial photographs (1:8 000, 1:10 000, and 1:40 000 scale).

Pits were used as a primary tool for measuring DTFG, since in the preliminary (1993) field season it was found that most DTFG values obtained by probe in the Mayo area cannot usually be assumed to be valid without confirmation by a pit. This is due to the inability of a field worker to identify with consistently high certainty the nature of any particular ground feature that may obstruct the passage of the steel probe through the ground. Ground features that may be confused with a frost table include tree roots, pebbles and cobbles, and firm clay layers.

Ground probing was performed to supplement pit measurements, as DTFG values can vary within an individual site. Probing was accomplished at those sites where it was deemed, based on pit stratigraphy, that the steel probe measurements would be valid DTFG measurements. At such sites, three individual probes were made at 5 m intervals in each of the four main compass directions, centred on the main site pit. Thus, 12 probe DTFG values supplemented the central pit DTFG measurement at these sites. This probing methodology was devised for efficiency and simplicity in field implementation.

Each site was assigned a single "best-estimate" DTFG number: either the pit value, or the average of the pit and probe measurements. DTFG values at a given site cluster around a small range of values, with occasional outliers due to drainage differences. Those sites where frozen ground was not found within 1.5 m of ground surface were given a best-estimate label of ">1.5 m, or absent."

CLASSIFICATION OF DEPTH TO LATE-SUMMER FROZEN GROUND

Classifiers Used

Three supervised classifiers were tested in this research: maximum likelihood, evidential reasoning, and a neural network. The **Maximum Likelihood (ML) classifier** was selected as it is the supervised classification method most commonly employed with remotely sensed imagery. The classification scheme involves the derivation, using training pixels, of distribution functions that characterize the attributes of each class within the multi-spectral space. The derivation of a given distribution function is based on the mean vector and covariance matrix that corresponds to the training data. It is assumed in ML that the probability distributions for the classes of interest are of the form of multi-variate normal models (Richards, 1993). The assumption usually precludes the use of nominal and ordinal levels as input data, since the Gaussian parameterization of such levels of data is invalid. ML is best suited for classification when used with continuous data types characterized by signature data with unimodal frequency distributions.

The **Evidential Reasoning (ER) classifier** is based on the derivation of a mass of evidence for a given set of all-encompassing class propositions, for a given source. The combination of evidence from more than one source is performed by employing Dempster's orthogonal sum. ER does not make statistical assumptions regarding probability distributions, and thus all information types (nominal, ordinal, interval, and ratio) are valid for use as classification sources (Peddle, 1993). ER can therefore handle both satellite imagery (ratio and continuous data) values and values corresponding to such discrete sources as land cover and surface geology (nominal and discontinuous data). Furthermore, ER can handle multi-modal signature distributions (those sometimes associated with aspect, for example). The ER software used here was written by the first author.

Unlike ER and ML, the operation of a **Neural Network (NN) classifier** is based on training-derived weight values associated with one-way vectors joining nodes ("neurons") within a network. Nodes within this network emulate biological neurons by taking input data from other nodes and performing simple operations on the data, selectively passing the results on to other nodes. The NN used here is commercially available from PCI Inc. as a module of EASI/PACE. The specific neural network system is a back-propagation network that uses the Generalized Delta Rule for learning (Maren *et al.*, 1990).

Classification Experiments

The classification experimental design consisted of five stages, involving the measurement of field data, the generation of imagery, the treatment of data, and the application and testing of the classifiers. DTFG field measurements were initially assigned to two active-layer classes, including one near-surface permafrost absence class. Then 240 site pixels were randomly selected from these measurements as training pixels for the classifiers. Each class was assumed to be fully represented spectrally in the training data. Third, a series of classifications was performed to test the ability of each classifier to classify the remaining 120 site pixels (the test pixels) correctly. The input included TM bands 3, 4, 5, NDVI, aspect, equivalent latitude, and land cover (**Figure 2**). Each classification used a different classifier and/or different combination of inputs. Fourth, additional classifications were performed for the purpose of testing the ability of the classifiers to predict three DTFG classes (including one frozen ground absence class). An 80/280 test/training ratio was used to include an appropriate number of training sites in the test (if the number of sources or classes is increased in a classification, so should the number of training sites be increased). Each classifier was tested using the most successful source combinations of stage 3. Fifth, the success of each DTFG classification was assessed in terms of the agreement between the proposed classes and the field-measured classes. This involved determining the percentage of test pixels that were labelled correctly for each classification. Results of the assessment of the two- and three-class tests were compiled in tabular form, and results for the three-class tests were also compiled as confusion matrices. Kappa (K) values (Rosenfield and Fitzpatrick-Lins, 1986) are not presented in this paper, as there is no clear evidence that the assumption of equal priors is valid here.

Of the seven datasets used in the study, five were deemed eligible for use with the ML classifier: equivalent latitude, NDVI, and TM bands 3, 4, 5. Land cover, a discrete data type, cannot be used with ML unless its classes can be arranged in a meaningful numerical order that is relevant to the classification at hand. Aspect usually cannot be used with ML due to its often multi-modal signature distributions, and aspect was therefore not used in the ML tests. Four different source combinations were used to test ML's ability to predict two active-layer classes. In the testing of the ER and NN classifiers, all seven data sources were considered to be eligible for input. Nine different source combinations were used to test the ability of these two classifiers to predict two active-layer classes.

Two hidden layers were utilized in all NN classifications. The number of nodes in each hidden layer for any particular classification varied depending on the number of sources used; a node number equal to a maximum of the number of sources used, or 2, was selected.

Results and Discussion

Two DTFG Classes

The results of 10 different combinations of inputs submitted to the classifiers, expressed in terms of per cent agreement between predicted and field-measured DTFG classes, are given in **Table 1**.

■ **Maximum Likelihood** — The agreement rate associated with the use of the NDVI source alone is 81%, while that associated with equivalent latitude is 67%. The strengths of these two sources are apparently complementary, since the best combination of sources used with the ML classifier in this study was found to be that including NDVI and equivalent latitude (agreement = 86%). The utility of these sources in ML active-layer class prediction should be expected, as NDVI and equivalent latitude are good indicators of land cover and maximum potential insolation, which are highly correlated with DTFG.

The combination of TM 3, 4, 5 and equivalent latitude produced an agreement rate of 85%. This combination requires less manipulation of imagery (employing TM bands 3, 4, 5 rather than NDVI), and thus might be a superior means through which different research teams can extract and combine DTFG imagery produced over different regions.

■ **Evidential Reasoning** — The aspect and equivalent latitude sources, when used alone, produced agreement rates of 53% and 68%, respectively. At first glance, aspect appears to contribute essentially nothing to the success of the DTFG classifications using ER. However, the agreement rate produced by aspect alone is not the best descriptor of classification utility: a slope of 0 was designated for the purposes of this study to represent zero evidence in all ER classifications, and thus the classifier left sites on flatlands unclass-

a)

b)

c)

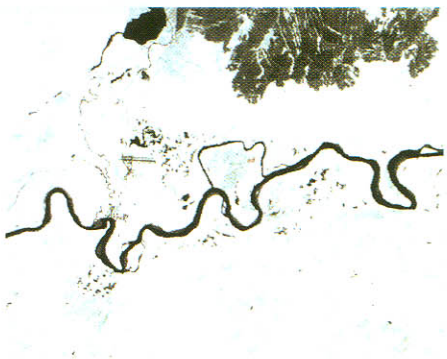

d)

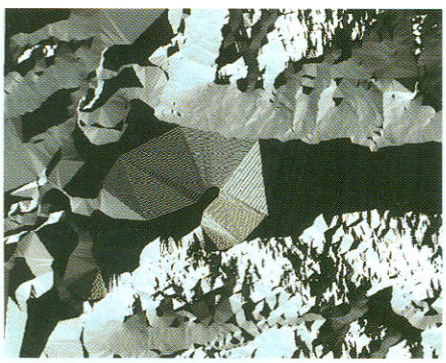

e)

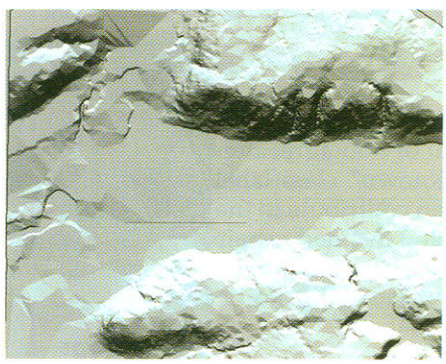

f)

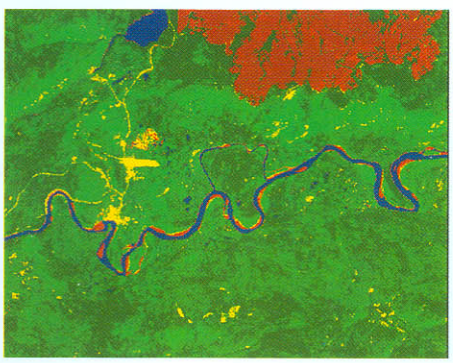

g)

Figure 2.
Input variables used in the classification experiments. TM bands a) 3, b) 4, and c) 5; d) NDVI; e) aspect; f) equivalent latitude; and g) land cover. The land cover classes (total of 13) have been grouped into fewer categories for displaying purposes only.

Table 1.
DTFG classification accuracies (two classes) using ML, ER, and NN classifiers on different combinations of variables derived from Landsat TM imagery and a DEM. Classifications that were not performed are denoted by an asterisk (*) (details are given in the text).

Variables	Maximum Likelihood % Agreement	Evidential Reasoning % Agreement	Neural Network % Agreement
1. NDVI	81	*	*
2. Aspect	*	53	71
3. Equivalent latitude	67	68	67
4. Land cover	*	85	81
5. NDVI, equivalent latitude	86	*	*
6. Land cover, aspect	*	85	87
7. Land cover, equivalent latitude	*	85	93
8. Land cover, equivalent latitude, aspect	*	85	93
9. TM 3, 4, 5, equivalent latitude	85	77	89
10. TM 3, 4, 5, equivalent latitude, aspect	*	78	87

ified. In this case, therefore, per cent agreement is not the opposite of per cent of non-agreement due to the presence of additional, "unknown" class labelling. Aspect used in this way with ER can contribute to the successful classification of sites located on inclined terrain units, and the lower agreement rate given here results from the distribution of test sites throughout the entire study area, a proportion of which is essentially flat.

The use of land cover produced the highest agreement rates of the ER classifier in this study. There was no increase in classification agreement (85%) when the land cover source was supplemented by other sources. The use of ER with the TM 3, 4, 5 and equivalent latitude combination produced an agreement rate of 77%. The addition of aspect to the four inputs increased classification agreement insignificantly to 78%.

■ **Neural Network** — Aspect and equivalent latitude were found to produce agreement rates of 71% and 67%, respectively. Land cover used alone produced a higher level of agreement, at 81%. The addition of other sources to land cover further increased agreement rates: the combination of land cover and aspect produced an agreement rate of 87%, and agreement rates of 93% were produced using the combination of land cover with equivalent latitude, and with equivalent latitude and aspect. The combination of TM bands 3, 4, 5 and equivalent latitude produced an agreement rate of 89%, while the addition of aspect to this combination produced an agreement rate of 87%. The NN results presented here vary slightly from those presented in Levering-ton and Duguay (1994), since the training dataset used in the earlier study was not as complete as that used here.

Table 2.
Classification accuracies for three DTFG classes.

Classifier	Variables	% Agreement
ML	NDVI, equivalent latitude	70
ER	Land cover, equivalent latitude, aspect	56
NN	Land cover, equivalent latitude	68

Table 3.
Confusion matrices for three DTFG classes using best combination variables (Shallow: < 70 cm; Deep: 70 cm ≤ DTFG ≤ 150 cm; Absent: no frozen ground).

a) ML

	Shallow	Deep	Absent	Total
Shallow	28	3	6	37
Deep	6	1	7	14
Absent	2	0	27	29
# test sites	36	4	40	80

b) ER

	Shallow	Deep	Absent	Total
Shallow	20	2	1	23
Deep	14	2	16	32
Absent	2	0	23	25
# test sites	36	4	40	80

c) NN

	Shallow	Deep	Absent	Total
Shallow	17	2	2	21
Deep	18	1	2	21
Absent	1	1	36	38
# test sites	36	4	40	80

Three DTFG Classes

The overall classification accuracies obtained using ML, ER, and NN for three DTFG classes, using the most successful source combinations for the prediction of two DTFG classes, are presented in **Table 2**. The confusion matrices for each test are given in **Table 3**, where the "shallow" class corresponds to a DTFG value of <70 cm, the "deep" class corresponds to a DTFG value of between 70 and 150 cm inclusive, and the "absent" class corresponds to an absence of frozen ground within 1.5 m of ground surface.

A 70% agreement rate was produced using the ML classifier. The ML confusion matrix indicates that erroneous differentiation between all three DTFG classes occurred. In the ML parameterization of the class signature functions, the deep DTFG class (the intermediate class) was assigned a class signature with elements in common with both shal-

low and unfrozen class signatures, producing the confusion seen here.

A 56% agreement rate was produced using the ER classifier. The ER confusion matrix indicates that the ER classifier made most errors in distinguishing between the shallow and deep DTFG classes, and the deep and absent classes (**Table 3b**). The confusion between the unfrozen class and the shallow DTFG class is minimal compared to that of the ML classification. Errors thus occurred mainly between adjacent classes.

A 68% agreement rate was produced using the NN classifier. The NN confusion matrix indicates that most confusion occurred between the two frozen DTFG classes (**Table 3c**). A higher rate of agreement in prediction of the unfrozen class (36 of 40 predicted correctly) was produced by the NN classifier. As with the previous two classifiers, however, the NN classifier did not predict three DTFG classes with an agreement rate approaching the 85–93% rates of the two-class classifications.

The much lower agreement rates of the classifiers in predicting three DTFG classes as compared to two DTFG classes is not surprising for this study area, given the field data presented in Leverington (1995a). The frozen DTFG values measured in the area appear to represent a single shallow class, with a small proportion of outliers to this class. The average value of the entire frozen DTFG dataset of the study area is 55 cm, and the standard deviation (SD) is 17 cm (the SD of the main distribution, ignoring the outliers, is of course lower). There are, therefore, apparently only two predominant near-surface DTFG classes in the study area (unfrozen, or frozen within a narrow depth range).

DTFG Imagery

Much of Canada's north is not mapped at high resolutions with regard to near-surface permafrost. The production of georeferenced data products based on the accurate extraction of DTFG classes would interest both Earth scientists and engineers. The regular production of relevant permafrost data products over large areas of Canada's north is a goal of the EOS CRYSYS program.

Based on the assessment of agreement between predicted and field-measured DTFG classes, the most accurate two-class data product generated in this study is that obtained with the NN classifier using land cover and equivalent latitude as input variables (with 93% agreement between predicted and field-measured DTFG classes). A high-resolution two-class data product based on the NN classification is shown in **Figure 3**. In the generation of the DTFG image, water bodies and a recently burned area, extracted from the land cover image, were overlain on the DTFG values. These land cover classes were added to the map both for reference purposes and to eliminate the (invalid) DTFG class predictions made for pixels associated with these land cover classes.

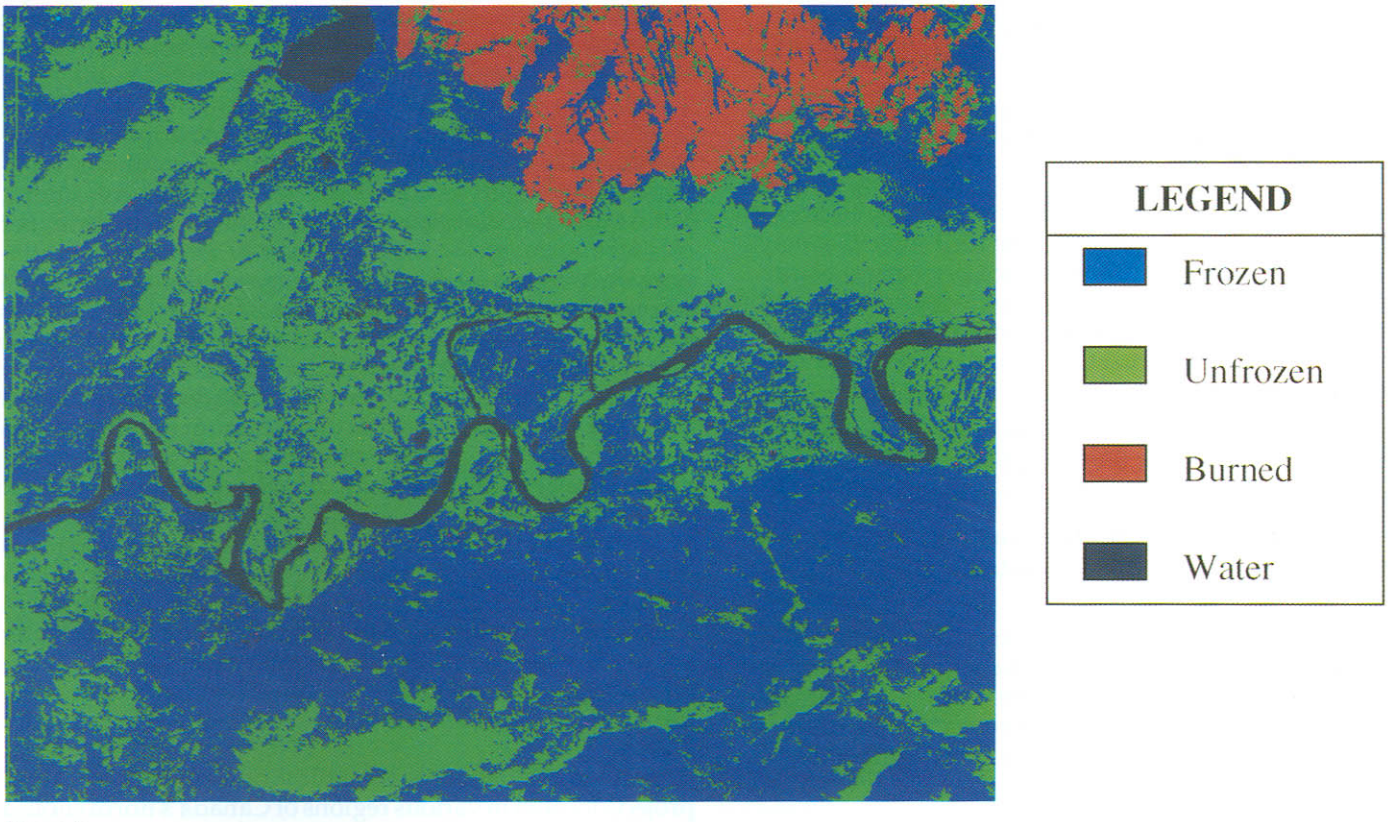

Figure 3.
Two-class DTFG image using the neural network classifier with land cover and equivalent latitude used as input variables.

Correlative Procedures as EOS CRYSYS Tools

The prediction of near-surface permafrost presence and absence using a correlative remote sensing methodology is possible in the Mayo region, using training data derived and employed within the confines of a small study area. The methods used in this study may be directly applicable to other areas within the discontinuous permafrost zone, particularly those with some relief (allowing for the inclusion of equivalent latitude as an important classification input). If positive results can be produced in a wide range of other northern areas, the prediction of DTFG conditions using remote sensing should evolve as a useful tool applicable to region-wide (central Yukon, for example) permafrost research and northern environmental management. In the future, DTFG imagery may be applicable toward climate and hydrological modelling of northern regions. The simplicity, reproducibility, high-resolution, and digital nature of the correlative remote sensing method is superior to other methods involving the use of climate-models or aerial photography, for example. The accuracy and utility of DTFG imagery produced using a correlative remote sensing methodology may increase over time, given the increases in remote sensing and computing power that are envisioned for the near future.

The long-term monitoring of near-surface permafrost using remote sensing has been identified within the EOS CRYSYS program as a possible manner in which to monitor aspects of global climate change. While imagery such as that produced here may find use in research and environmental management as discussed above, climate monitoring does not currently appear to be best performed using correlative permafrost models and remote sensing imagery, for the following reasons:

- the vertical resolution of near-surface DTFG classes produced in this study is not sufficiently fine for detecting change over time;
- there is necessarily a significant time lag between change in climate and the change in land cover that may result from changes in near-surface permafrost conditions (this time lag may be on the order of decades, and land cover changes are furthermore likely to be characterized by "noise" due to other natural forcing phenomena);
- over time, land cover-permafrost correlative relationships may change at a given study area, requiring the resampling of active-layer thicknesses; and
- depending on the portability of training data, the costs of measuring DTFGs over a large region could well prove to be prohibitively high.

The simplicity and accuracy of monitoring surface and borehole temperatures and permafrost conditions *in situ* at a wide range of sites across northern regions for climate change monitoring thus appears at this time to be an attractive alternative to correlative remote sensing models of DTFG.

CONCLUSIONS AND FUTURE RESEARCH

Three main conclusions can be drawn from this research:

- *Satellite imagery and topographic data can be used to coarsely classify near-surface permafrost conditions within the boreal forest of central Yukon.* All three classifiers (ML, ER, and NN) produced best results equal to or above 85% agreement between predicted and field-measured frozen ground presence and absence. Particularly effective source combinations involved the inclusion of land cover (or analogous sources: NDVI or TM bands 3, 4, 5) and equivalent latitude.

- *The NN classifier produced the highest two-class DTFG classification agreement.* A 93% agreement rate resulted from the use of the NN classifier and the source combination of land cover and equivalent latitude. Because of the NN classifier's ease of use, its multi-source capabilities, its commercial availability, and its strength in producing DTFG classifications characterized by high agreement rates between predicted and field-measured DTFG classes, the NN classifier may be particularly appropriate for use in future DTFG prediction studies in central Yukon or elsewhere in the discontinuous permafrost zone.

- *Agreement rates of 70%, 56%, and 68% were produced in three-class DTFG classifications, produced by the ML, ER, and NN classifiers, respectively.* The decrease in classification accuracies as compared to the two-class results is due either to the inability of the classifiers to discriminate between three real DTFG classes or, more likely, to the fact that there are only two primary near-surface late-summer DTFG classes present in the study area.

Much work remains regarding the application of correlative classification schemes toward the generation of high-resolution imagery of near-surface permafrost conditions. Future focus on determining the typical minimum number of sites necessary for the prediction of permafrost conditions may be useful. The field component of this research focused on visiting the maximum possible number of sites to ensure the availability of a valid training dataset; a lower number of well-distributed and representative training sites may have been sufficient to produce good classification results. It should be noted that the minimum number of sites necessary for DTFG classifications at a given study area may not be similar to the minimum number of sites necessary at other study sites.

More generally, future permafrost research should focus on understanding the nature of permafrost and DTFG values in various regions of Canada's north. Few areas in Canada's discontinuous permafrost zone have been fully surveyed with regard to late-summer near-surface DTFG, for example. Thus, typical DTFG characteristics of areas in Canada's discontinuous permafrost zone are not well known.

Further evaluation of the utility of classifiers in DTFG projects located in various regions of Canada's north should be performed; the utility of a given classifier may change from region to region, as the quantitative and correlative

characteristics of training data change. An evaluation of the utility of various source combinations in different DTFG projects is also necessary. As well, the utility of a given source combination may change from region to region, and new sources may be applicable toward permafrost studies. The use of residual snow patch imagery may be particularly useful in DTFG classifications made for relatively flat areas, since equivalent latitude must have much less impact than snow accumulation in determining near-surface permafrost conditions at these areas. Land cover classifications based on multi-season satellite imagery may further aid in the discrimination of the surface classes that are strongly related to near-surface permafrost conditions, potentially improving DTFG classifications. Imagery produced by satellite and airborne radar sensors may provide useful information on ground moisture and the phase-state of ground materials.

The topic of training data portability in DTFG classification must be addressed if the need for complete field-sampling of large northern regions is to be avoided. A second study area in the Mayo region was sampled by the authors in late summer of 1994, and was used in a preliminary experiment of training data portability in the Mayo region. The results of this experiment will be presented in an upcoming paper.

Acknowledgements

This research was supported by scholarships from the Natural Sciences and Engineering Research Council of Canada (NSERC) to D. Leverington and research grants from the Atmospheric Environment Service (AES) and NSERC to C. Duguay. Additional support was provided by two Department of Indian and Northern Affairs NSTP field work grants to D. Leverington. The Landsat TM image was kindly provided by Dr. Kian Fadaie of the Canada Centre for Remote Sensing (CCRS) in support of NASA's EOS CRYSYS program. Thanks are due Dr. Toni Lewkowicz, Dr. Chris Burn, and Dr. Graeme Bonham-Carter for their help in many aspects of this study. We are indebted to Geraldine Bergmans and Phil Wilson for their enthusiastic assistance in the field. The helpful comments of two anonymous reviewers are appreciated.

References

Anderson *et al.* 1973. *Arctic and Subarctic Environmental Analysis Utilizing ERTS-1 Imagery*. NASA, Report E74-10017/CR-13585.

Beaubien, J. 1994. "Landsat TM Satellite Images of Forests: From Enhancement to Classification," *Canadian Journal of Remote Sensing*, Vol. 20(1), pp. 17–26.

Bostock, H.S. 1946. *Mayo, Yukon Territory, Map 890A*. Geological Survey of Canada.

Bostock, H.S. 1966. *Notes on Glaciation in Central Yukon Territory*. Geological Survey of Canada, Paper 65-36.

Brown, R.J.E. 1967. *Permafrost Investigations in British Columbia and Yukon Territory*. Division of Building Research, National Research Council of Canada, Technical Paper 253.

Brown, R.J.E. 1978. "Permafrost," *Hydrological Atlas of Canada*. Ottawa: Fisheries and Environment Canada, Plate 32.

Burn, C.R. 1985. *Guidebook to the Surface Geology and Environmental History of the Silver Trail*. Mayo, Yukon Territory: Silver Trail Tourism Association.

Burn, C.R. 1991. "Permafrost and Ground Ice Conditions Reported During Recent Geotechnical Investigations in the Mayo District, Yukon Territory," *Permafrost and Periglacial Processes*, Vol. 2, pp. 259–268.

Burn, C.R. 1994. "Permafrost, Tectonics and Past and Future Regional Climate Change, Yukon and Adjacent Northwest Territories," *Canadian Journal of Earth Sciences*, Vol. 31, pp. 182–191.

Burn, C.R. and P.A. Friele. 1989. "Geomorphology, Vegetation Succession, Soil Characteristics, and Permafrost in Retrogressive Thaw Slumps Near Mayo, Yukon Territory," *Arctic*, Vol. 42, pp. 31–40.

Burn, C.R. and M.W. Smith. 1990. "Development of Thermokarst Lakes During the Holocene at Sites Near Mayo, Yukon Territory," *Permafrost and Periglacial Processes*, Vol. 1, pp. 161–176.

Cihlar, J., L. St-Laurent, and J.A. Dyer. 1991. "Relation Between the Normalized Vegetation Index and Ecological Variables," *Remote Sensing of Environment*, Vol. 35, pp. 279–298.

CRYSYS Steering Committee. 1991. *Science Report on the CRYSYS Workshop for University Investigators*. Report ISTS-EOL-TR92-003, Institute for Space and Terrestrial Science, University of Waterloo.

Ferrians, O.J. and G.D. Hobson. 1973. "Mapping and Predicting Permafrost in North America: A Review, 1963–1973," *Proceedings of the Second International Permafrost Conference*, National Academy Press, Washington, D.C., pp. 479–498.

Gabrielse, H., D.J. Tempelman-Kluit, S.L. Blusson, and R.B. Campbell. 1980. *MacMillan River: Yukon, District of Mackenzie, Alaska*. Map 1398A, Map Sheet 105-115, 1:1 000 000, Geological Atlas, Geological Survey of Canada.

Hall, D.K. and J. Martinec. 1985. *Remote Sensing of Ice and Snow*. London, England: Chapman and Hall Ltd.

Hughes, O.L. 1983. *Surficial Geology and Geomorphology, Janet Lake*. Map 4-1982, Geological Survey of Canada.

Hughes, O.L., N.W. Rutter, and J.J. Clague. 1989. "Yukon Territory (Quaternary Stratigraphy and History, Cordilleran Ice Sheet)," *Quaternary Geology of Canada and Greenland*, R.J. Fulton (ed.), Geological Survey of Canada, Geology of Canada, No. 1, pp. 58–61.

Leverington, D.W. 1995a. "A Field Survey of Late-Summer Depths to Frozen Ground at Two Study Areas Near Mayo, Yukon Territory, Canada," *Permafrost and Periglacial Processes*, in press.

Leverington, D.W. 1995b. *Prediction of Depth to Late-Summer Frozen Ground Using Satellite Imagery and Digital Topographic Data, Mayo, Yukon Territory*. Unpublished MSc. Thesis, Ottawa-Carleton Geoscience Centre, Department of Geology, University of Ottawa.

Leverington, D.W. and C.R. Duguay. 1994. "Application of a Neural Network Toward Mapping Near-Surface Active-Layer Thickness," *Proceedings of the Seventeenth Canadian Symposium on Remote Sensing*, Vol. I, Canadian Remote Sensing Society, pp. 47–51.

Maren A.J., C.T. Harston, and P.M. Pap. 1990. *Handbook of Neural Computing Applications*. San Diego: Academic Press.

Morrissey, L.A. 1984. "Multisensor Analysis of Environmental Factors in Alaska," *Proceedings of the Ninth Canadian Symposium on Remote Sensing*, Canadian Remote Sensing Society, pp. 653–661.

Morrissey, L.A., L. Strong, and D.H. Card. 1986. "Mapping Permafrost in the Boreal Forest with Thematic Mapper Satellite Data," *Photogrammetric Engineering and Remote Sensing*, Vol. 52, pp. 1513–1520.

NRC. 1988. *Glossary of Permafrost and Related Ground-Ice Terms*. Permafrost Subcommittee, Associate Committee on Geotechnical Research, National Research Council of Canada.

Peddle, D.R. 1993. "An Empirical Comparison of Evidential Reasoning, Linear Discriminant Analysis, and Maximum Likelihood Algorithms for Alpine Land Cover Classification," *Canadian Journal of Remote Sensing*, Vol. 19(1), pp. 31–44.

Peddle, D.R. and S.E. Franklin. 1993. "Classification of Permafrost Active Layer from Remotely Sensed and Topographic Evidence," *Remote Sensing of Environment*, Vol. 44, pp. 67–80.

Peddle, D.R., G.M. Foody, A. Zhang, S.E. Franklin, and E.F. LeDrew. 1994. "Multi-source Image Classification II: An Empirical Comparison of Evidential Reasoning and Neural Network Approaches," *Canadian Journal of Remote Sensing*, Vol. 20(4), pp. 396–407.

Richards, J.A. 1993. *Remote Sensing and Digital Image Analysis*. New York: Springer-Verlag.

Rosenfield, G.H. and K. Fitzpatrick-Lins. 1986. "A Coefficient of Agreement as a Measure of Thematic Classification Accuracy," *Photogrammetric Engineering and Remote Sensing*, Vol. 52, pp. 223–227.

Scott, A.J. 1995. *Canada's Vegetation: A World Perspective*. Montreal and Kingston: McGill-Queen's University Press.

Tarnocai, C. and J. Thie. 1974a. "Application of Remote Sensing to Permafrost Studies," *Conference in Permafrost Hydrology and Geophysics*, Feb. 25–28, Calgary, Alberta, pp. 1–5.

Tarnocai, C. and J. Thie. 1974b. "Permafrost and Remote Sensing," *Proceedings of the Second Canadian Symposium on Remote Sensing*, Guelph, Canadian Remote Sensing Society, Ottawa, Vol. 2, pp. 438–447.

Wahl H.E., D.B. Fraser, R.C. Harvey, and J.B. Maxwell. 1987. *Climate of Yukon*. Environment Canada, Atmospheric Environment Service.

Williams, P.J and M.W. Smith. 1989. *The Frozen Earth: Fundamentals of Geocryology*. New York: Cambridge University Press.